# THERMODYNAMIC ASSESSMENT OF THE Cu-In-Se SYSTEM AND APPLICATION TO THIN FILM PHOTOVOLTAICS

C.H.Chang, A. Davydov , B.J. Stanbery and T.J. Anderson

Department of Chemical Engineering, University of Florida, Gainesville, FL 32611

## Abstract

A critical assessment of the thermochemical and phase diagram data for the Cu-In-Se system has been initiated. This report includes assessment of the Se unary, In-Se binary and Cu-Se binary systems. Based on these assessments and a previously published one [7] for the Cu-In system a preliminary evaluation of the the $Cu_2Se$-$In_2Se_3$ pseudobinary phase diagram is proposed. The results of these analyses were applied to the calculation of the flux from a selenium effusion cell used for depositing CIS films and to the prediction of crystallization pathways during annealing of CIS precusor films.

## Introduction

Considerable progress has recently been achieved in CIS-based solar cell technology. This progress has been achieved in part, through innovation in materials processing, although the processes are not optimized or fully understood. A starting point for understanding the reaction pathways in CIS processing is to examine the phase equilibria in the Cu-In-Se system. Performing an assessment of a multicomponent system begins with assessment of the unary and binary systems. These are the most critical assessments since most of the phases present in the multicomponent system are also contained in the binary ones and the fluid phase interactions are present as well. Standard CALPHAD (CALculation of PHAse Diagrams) procedures were used in the critical evaluation, including application of the Lukas [1] and ThermoCalc [2] software systems. The assessment was initiated with an examination of the unary Se system and gas phase non-idealities were accounted for using the Peng-Robinson equation of state. The In-Se and Cu-Se binary systems were then assessed using a Redlich-Kister expansion to describe their liquid mixture behavior. The input to this assessment process consists of thermodynamic properties of the compounds (e.g., $\Delta H_{f298}$, $C_p$), solution data (e.g., $\Delta H_{mix}$, component activities), and phase equilibria data (e.g., liquidus, solidus, vapor pressures). The output is optimized expressions for the Gibbs energy of each phase, which can be used to calculate phase diagrams, equilibrium vapor pressures, and component chemical potentials.

## Selenium unary system

The stable solid phase of selenium exhibits a hexagonal structure and melts at 494.3 K. The liquid phase of pure selenium is complex due to vibrational energy contributions, free volume effects, and both ring-chain and depolymerization reactions. Like sulphur, selenium exhibits a complex structure in the vapor phase. Mass-spectrometric measurements have shown the presence of each of the molecular species from the monomer to $Se_{10}$, the more abundant ones being $Se_2$ through $Se_8$. Studies of the molecular composition of selenium vapor have been performed using a variety of methods. These include vapor density, optical absorption, torsion and Knudsen effusion measurements, and mass-spectrometry.

**Figure 1**

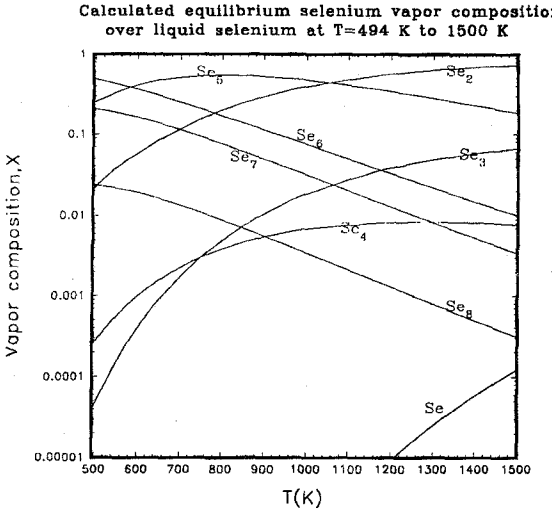


The assessment of the thermodynamic properties of Se(c,hexagonal), Se($\ell$) and $Se_n$(g) {n=1-8} resulted in suggested values for $\Delta H_{f,298}$, $S^\circ_{298}$, and $C_p(T)$ . The thermodynamic functions of the gaseous phase were assessed from literature data or calculated from molecular constants assuming harmonic oscillator, rigid rotor and ideal gas behavior. Second and third law analyses were performed on literature data to assess values of $\Delta H_{f,298}$ for $Se_n$(g). The values of $\Delta H_{f,298}$ for $Se_5$(g) and $Se_6$(g) were optimized using the vapor pressure measured in equilibrium



0-7803-3166-4/96/$5.00 © 1996 IEEE

with Se(ℓ) and Se(c,hexagonal), respectively. Gas phase nonidealities were taken into account by using the Peng-Robinson equation of state. The result of this assessment is an expression for the Gibbs energy of each of the ten species Se(c,hexagonal), Se(ℓ) and $Se_n$(g) {n=1-8} as a function of temperature. These expressions were then used to calculate equilibria in the Se system. Fig.1 shows the calculated gas phase compositions above liquid Se. It is interesting to note that the predominant species at a temperature above approximately 1000 K is the dimer, while at a lower temoerature (~600-1000K) $Se_5$(g) is the dominant species. Below 600K $Se_6$(g) is the major species. During growth from a Se evaporation source, a change in deposition chemistry might be expected as the temperature is changed through this transition.

## In-Se binary system

The phase diagram and thermochemistry of the In-Se system has been experimentally investigated by several authors and the results for selected properties are inconsistent. Early studies(3) performed by DTA and X-ray analyses reported four intermediate compounds ($In_2Se$, InSe, $In_5Se_6$ and $In_2Se_3$), with InSe and $In_2Se_3$ identified as congruently melting compounds. A miscibility gap on the In-rich side of the phase diagram was also suggested. Later investigators (4,5) reported the existence of the four compounds $In_4Se_3$ (instead of $In_2Se$), InSe, $In_6Se_7$ (instead of $In_5Se_6$) , and $In_2Se_3$ , with only the $In_2Se_3$ melting congruently. In addition, liquid-liquid miscibility gaps on both sides of the phase diagram were observed. Experimental measurements of $\Delta H_{f,298}$ are available for each compound. Both low and high temperature heat capacity measurements have been reported for each compound with the exception of $In_4Se_3$. The complete database for the In-Se system was assembled and selected data analyzed in view of changes in the compound stoichiometry and the Se vapor thermodynamic properties. The selected database was combined with the unary data for indium from the SGTE database [6] and the assesssed Se data previously discussed. The resulting experimental data were assigned uncertainties and then optimized using the BINGSS routine [1]. In this procedure, the parameters describing the temperature dependence of the Gibbs energy of the liquid solution were optimized using a maximum likehood algorithm.

**Figure 2**

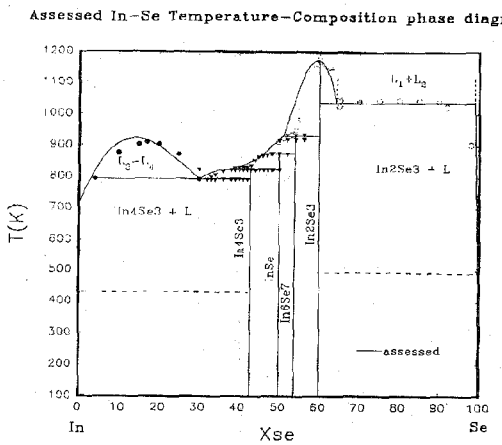


The phase stability expressions for the pure indium and selenium are given relative to the Standard Element Reference (SER) as follows,

$$G\text{-}H_{SER} = A + BT + CT\ln T + DT^2 + ET^3 + F/T + GT^7 + HT^{-9}$$

Each compound in the In-Se system was treated as stoichiometric compound and modeled as follows,

$$G\text{-}H_{SER} = A + BT + CT\ln T + DT^2 + ET^3 + F/T$$

The Redlich-Kister polynomial expression for the Gibbs energy of liquid phase has the form,

$$G - H^{SER} = ( {}^0G_{In} - {}^0H_{In}^{SER} )\, x_{In} + ( {}^0G_{Se} - {}^0H_{Se}^{SER} )\, x_{Se} + RT ( x_{In} \ln x_{In} + x_{Se} \ln x_{Se} ) + x_{In}\, x_{Se} \sum_{v=0}^{n} K_v ( x_{In} - x_{Se} )^v$$

where the Kv are functions of temperature, fitted to

$$K_v = a_v + b_v T + c_v T \ln T + \ldots$$

An assessment of the In-Se system was performed using these models to describe each phase. Good agreement with the selected experimental data was found. Figure 2 shows the assessed phase diagram (solid/dashed lines) and compares the calculated phase diagram to the experimental measurements. Four line compounds were included with only $In_2Se_3$ melting in a congruent fashion. The optimized

**Table 1. Assessed G-$H_{SER}$ for intermediate compounds in the In-Se system**

| Phase | Temperature range [K] | G-$H_{SER}$ [J/ K mol] |
|---|---|---|
| $In_2Se_3$ | 298.15 - 486 | -310173.88 + 574.22947 T -111.91908 TlnT - 2.0645x10$^{-2}$T$^2$ |
| | 486 - 623 | -307174.72 + 595.48792 T - -116.8701 TlnT -1.406x10$^{-2}$T$^2$ |
| | 623 - 1023 | -297323.47 + 486.52411T - 101.10952 TlnT - 2.732x10$^{-2}$T$^2$ |
| | 1023 - 1072.58 | -316394.26 + 871.49704 T -158 TlnT |
| $In_6Se_7$ | 298.15 - 928.78 | -799600.36 + 1807.69511T -347.57273 TlnT + 3.34152x10$^{-2}$T$^2$ - 2.0713316x10$^{-5}$T$^3$ + 558409.08/T |
| InSe | 298.15 - 873.16 | -110095.98+260.75476T- 52.32 TlnT +3.14x10$^{-3}$T$^2$ - 1.4x10$^{-6}$T$^3$+ 89500/T |
| $In_4Se_3$ | 298.15 - 823.26 | -375360.37+1041.07773T-196.627 TlnT -1.2118x10$^{-2}$T$^2$ + 1464400/T |

*Gibbs energy expressions* for the intermediate compounds are listed in Table 1.

## Cu-Se system

**Figure 3**

Assessed Cu-Se Temperature-Composition phase diagram

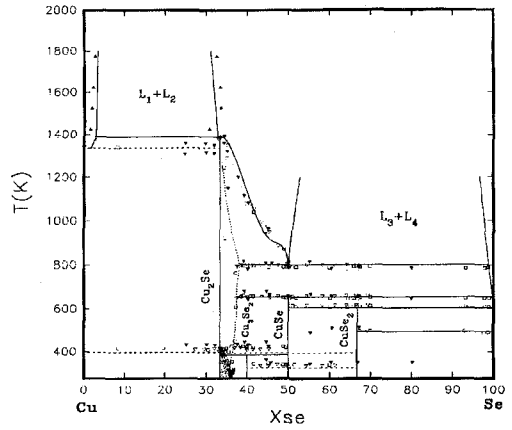


The phase diagram for Cu-Se system includes a liquid phase which exhibits two miscibility gaps, one for Cu-rich compositions and the other on the Se-rich side of the phase diagram. Four intermediate phases were reported in the literature, including $Cu_2Se$/ $Cu_{2-X}Se$, $Cu_3Se_2$, CuSe, and $CuSe_2$ . The $Cu_2Se$/ $Cu_{2-X}Se$ phase was the most stable phase in this system with a broad homogeneity range extending into the Se side to form a defect compound. Extensive work has been conducted to clarify the Cu-Se phase diagram by means of DTA, Xray, microscopy and microhardness techniques. These data are in qualitative agreement. Chakrabarti and Laughlin [8] reviewed the phase diagram and thermodynamic data for the system, but did not perform an optimized assessment.

We have performed a preliminary assessment of the Cu-Se system using the Redlich-Kister model to describe the liquid phase behavior. Four intermediate solid phases ($Cu_2Se$, $Cu_3Se_2$, CuSe, $CuSe_2$) were modeled as line compounds. Experimental data for $\Delta H_{f,298}$ and $S^{\circ}_{298}$ are available for each compound. Only the heat capacity data for $Cu_2Se$ are available in the literature. The heat capacity data for $Cu_3Se_2$, CuSe, and $CuSe_2$ were estimated using the Unäl-Kubaschewski rule [9] and corrected by applying the same rule to $Cu_2Se$. The resulting data were assigned uncertainties and the same BINGSS routine [1] was applied to optimize these parameters. Excellent agreement between the assessment and experimental phase diagram was found. As seen in Fig. 3, four line compounds were included with only $Cu_2Se$, melting in a congruent fashion (at 1393.51K). The vapor species in equilibrium with the condensed phases in the Cu-Se system are Cu(g), $Se_n$(g), CuSe(g), and $Cu_2Se$(g), with $Se_2$(g) the most prominent species. The assessed $Se_2$ partial pressure in equilibrium with the liquidus, $Cu_2Se$, CuSe, and $CuSe_2$ is given in Fig. 4 together with the experimental data. Good agreement is achieved between the calculated T-p curve and the experimental data [10].

**Figure 4**

Assessed T-p phase diagram for Cu-Se system

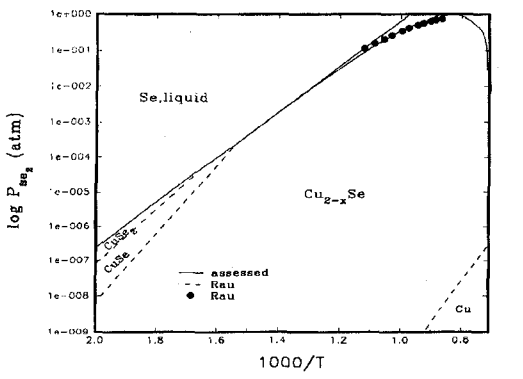


## The $Cu_2Se$-$In_2Se_3$ pseudobinary system

Each ternary compound formed in the Cu-In-Se system occurs along the $Cu_2Se$-$In_2Se_3$ compositional tie-line. We have made a tentative evaluation of the T-x diagram for this pseudobinary section. Sufficient evidence for the existence of the $Cu_5InSe_4$ and $Cu_3In_5Se_9$ phases was not found, which were previously deduced solely from thermal analysis data. Phases α and δ in Fig. 5 are domains of chalcopyrite and sphaelerite crystal structures, respectively. Phase β is referred to in the literature as comprised of 3 compounds, $Cu_2In_4Se_7$, $Cu_8In_{18}Se_{32}$ and $Cu_7In_{19}Se_{32}$, but is considered by the present authors to be a defect chalcopyrite structure of solid solutions within a composition range bounded by the compounds $Cu_2In_4Se_7$ and $CuIn_5Se_8$. Phase relations in the 80-100 mol.% $In_2Se_3$ region are much less well defined.

**Figure 5**

Evaluated $Cu_2Se$-$In_2Se_3$ pseudobinary phase diagram

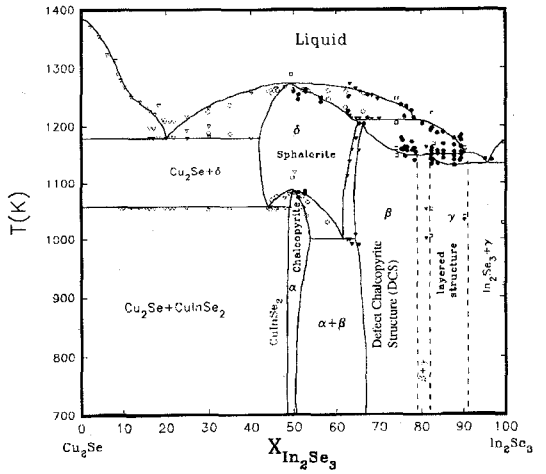


In Fig. 5 the $CuIn_5Se_8$ compound is tentatively included in the γ phase homogeneity region, described in [11] as a solid solution with layered structure, stable in the 82-92 mol % $In_2Se_3$ range. Once additional experimental and thermodynamically assessed data on ternary compounds and phase relations become available, a more reliable T-x

diagram of the $Cu_2Se$-$In_2Se_3$ and other sections in the Cu-In-Se system can be evaluated.

## Applications

The results of our Se assessment are applied to calculate the Langmuir evaporation flux that can be useful in characterizing the performance of an evaporation source. The Hertz-Langmuir equation

$$J_{Se_n} = \alpha N_A P_{Se_n} / \sqrt{2\pi M_{Se_n} RT}$$

was used, where

$\alpha$ = evaporation coefficient

$N_A$ = Avogadro's number

$P_{Se_n}$ = partial pressure of $Se_n(g)$

$M_{Se_n}$ = molecular weight of $Se_n(g)$

The evaporation coefficients for $Se_n(g)$ were studied by Huang *et al* [12]. The data were assessed by Drowart *et al* [13] who determined that $\alpha$ = 0.23 for each of the $Se_n(g)$ species, a result adopted for this calculation as well as the assumption that the temperature dependence of $\alpha$ is negligible. The results are given in Fig. 6.

**Figure 6**

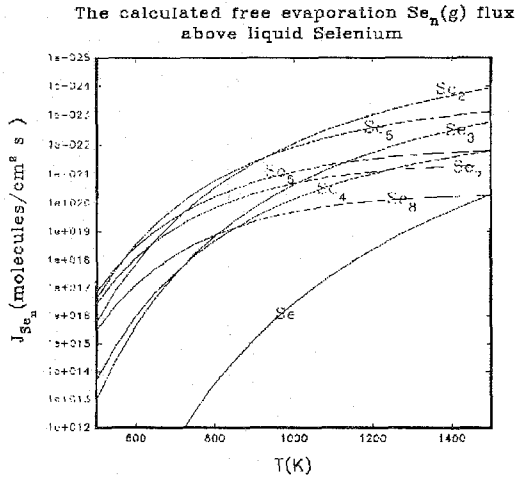


The predominance diagram for In-Se system is produced from the assessed Gibbs energy functions listed in Table 1. It shows the thermodynamically stable phase in each range of temperature and selenium pressure, and is shown in Fig.7.

## Conclusion

A critical assessment of the thermochemical and phase diagram data for the Cu-In-Se system using standard CALPHAD procedures has begun with the Se unary and binary In-Se and Cu-Se systems. The $Cu_2Se$-$In_2Se_3$ pseudobinary phase diagram has been re-examined. The results of this assessment have been applied to the calculation of the flux characteristics of Langmuir cells for selenium evaporation, and to the engineering of precursor films for CIS synthesis. The next steps in this process will be the critical assessment of the $Cu_2Se$-$In_2Se_3$ pseudobinary section and union of the three binary assessments to predict the phase relations along other pseudobinary tie-lines in the ternary phase field. Experimental studies of the phase diagrams and liquid mixture behaviors in the Cu-In-Se system are also underway in our laboratories. These experiments will test the assessment and substantiate the database used in the optimization.

**Figure 7**

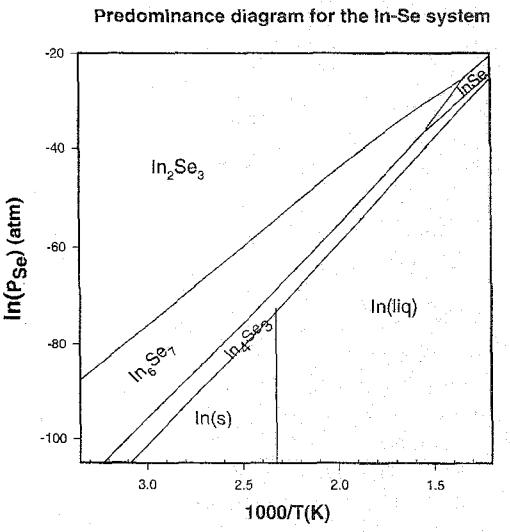



## Acknowledgements

The authors would like to acknowledge support of this work by National Renewable Energy Laboratory under contract No. XAF-5-14142-10 and to Dr. H.L. Lukas for the provision of the optimization program, BINGSS.


## References


[1]. H.L.Lukas, B.G. Fries, *J. Phase Equilbria*, **13**, 532,1992

[2]. B. Sundman *et al*, *Calphad*, **9**, 153, (1985)

[3].G. K. Slavnova, N.P. Luzhnaya, Z.S. Medvedeva, *Russ. J. Inorg. Chem.*, **8**(5),78,(1963) ].

[4]. A. Likforman, M. Guittard, *Compt. Rend. (Paris) C*, **279**, 33, (1974)

[5]. K. Imai, K. Suzuki, Y. Hazegawa and Y. Abe, *J. Crystal Growth*, **54**, 501 (1981)

[6]. A. T. Dinsdale, *CALPHAD*, **15**, 317, (1991)

[7]. C.R. Kao *et al*, *J. Phase Equil.*,**14**, 22, 1993

[8]. D. J. Chakrabarti, D. E. Laughlin, *Bulletin of Alloy Phase Diagrams*, **2**(3), 305, 1981

[9].O. Kubaschewski,H. Unäl ,*High Temp. High Pressure*, **9**, 361, (1977)

[10].H. Rau, A. Rabenau, *J. Sol. St. Chem.*, 1, 515, (1970)

[11].U.C. Boehnke, G. Kühn, *J. Mater. Sci.*, **22**,1653, (1987)

[12].J.Y.K. Huang , p. W. Gilles, J.E. Bennett, *High Temp. Sci.*, **17**,109, (1984)

[13].J. Drowart, S. Smoes, A. M. Vander Auwera-Mahieu, E. *Trio, Procs.,3rd Int'l Symp. Industrial uses of Se and Te.* (Saltsjöbaden, Sweden 1984)